AD

TECHNICAL REPORT ARCCB-TR-02009

CHARACTERIZATION OF STEELS USING A REVISED KINEMATIC HARDENING MODEL INCORPORATING BAUSCHINGER EFFECT

ANTHONY P. PARKER
EDWARD TROIANO
JOHN H. UNDERWOOD
CHARLES MOSSEY

AUGUST 2002

US ARMY ARMAMENT RESEARCH,
DEVELOPMENT AND ENGINEERING CENTER
Close Combat Armaments Center
Benét Laboratories
Watervliet, NY 12189-4000

TACOM-ARDEC

BENÉT LABS

APPROVED FOR PUBLIC RELEASE; DISTRIBUTION UNLIMITED

DISCLAIMER

The findings in this report are not to be construed as an official Department of the Army position unless so designated by other authorized documents.

The use of trade name(s) and/or manufacturer(s) does not constitute an official endorsement or approval.

DESTRUCTION NOTICE

For classified documents, follow the procedures in DoD 5200.22-M, Industrial Security Manual, Section II-19, or DoD 5200.1-R, Information Security Program Regulation, Chapter IX.

For unclassified, limited documents, destroy by any method that will prevent disclosure of contents or reconstruction of the document.

For unclassified, unlimited documents, destroy when the report is no longer needed. Do not return it to the originator.

REPORT DOCUMENTATION PAGE

Form Approved
OMB No. 0704-0188

1. AGENCY USE ONLY *(Leave Blank)*	2. REPORT DATE August 2002	3. REPORT TYPE AND DATES COVERED Final

4. TITLE AND SUBTITLE
CHARACTERIZATION OF STEELS USING A REVISED KINETIC HARDENING MODEL INCORPORATING BAUSCHINGER EFFECT

5. FUNDING NUMBERS
AMCMS No. 6226.24.H180.0
PRON No. TU1G1F261ABJ

6. AUTHORS
Anthony P. Parker (Royal Military College of Science, Cranfield University, Swindon, UK),
Edward Troiano, John H. Underwood, and Charles Mosey

7. PERFORMING ORGANIZATION NAME(S) AND ADDRESS(ES)
U.S. Army ARDEC
Benet Laboratories, AMSTA-AR-CCB-O
Watervliet, NY 12189-4000

8. PERFORMING ORGANIZATION REPORT NUMBER
ARCCB-TR-02009

9. SPONSORING / MONITORING AGENCY NAME(S) AND ADDRESS(ES)
U.S. Army ARDEC
Close Combat Armaments Center
Picatinny Arsenal, NJ 07806-5000

10. SPONSORING / MONITORING AGENCY REPORT NUMBER

11. SUPPLEMENTARY NOTES
To be presented at Gun Tubes Conference 2002, Keble College, Oxford, UK, 15-18 September 2002.
To be published by *ASME Journal of Pressure Vessel Technology*.

12a. DISTRIBUTION / AVAILABILITY STATEMENT
Approved for public release; distribution unlimited.

12b. DISTRIBUTION CODE

13. ABSTRACT *(Maximum 200 words)*

A new variant of the nonlinear kinematic hardening model is proposed that accommodates both nonlinear and linear strain hardening during initial tensile loading and reduced elastic modulus during initial load reversal. It also incorporates the Bauschinger effect, as a function of prior tensile plastic strain, during the nonlinear compressive loading phase. The model is shown to fit experimental data from a total of five candidate gun steels. The numerical fits will be employed in subsequent work to predict residual stresses and fatigue lifetimes for autofrettaged tubes manufactured from the candidate steels.

14. SUBJECT TERMS
Kinetic Hardening Model, Elastic Modulus, Bauschinger Effect, Autofrettage, Steels,
A723 Steel, HY180 Steel, PH 13-8 Mo Steels, Residual Stress, Pressure Vessels, Gun Tubes

15. NUMBER OF PAGES
16

16. PRICE CODE

17. SECURITY CLASSIFICATION OF REPORT	18. SECURITY CLASSIFICATION OF THIS PAGE	19. SECURITY CLASSIFICATION OF ABSTRACT	20. LIMITATION OF ABSTRACT
UNCLASSIFIED	UNCLASSIFIED	UNCLASSIFIED	UL

NSN 7540-01-280-5500

Standard Form 298 (Rev. 2-89)
Prescribed by ANSI Std. Z39-1
298-102

TABLE OF CONTENTS

TABLES

LIST OF ILLUSTRATIONS

ACKNOWLEDGEMENTS

The first author (Anthony P. Parker) gratefully acknowledges support from the U.S. Army Armament Research, Development and Engineering Center, Watervliet, NY, and from the European Research Office of the U.S. Army Research, Development and Standardization Group, UK.

INTRODUCTION

Accurate numerical analyses of stress and strain in steel pressure vessels, including gun tubes, require high quality uniaxial stress-strain data and an accurate numerical fit to such data. A detailed overview is given in Reference 1. These data then provide the equivalent stress input to yield criteria, such as von Mises and Tresca, for the numerical solution of two-dimensional and three-dimensional configurations. A serious omission from published numerical fitting procedures is any consistent and reliable method for representing the behavior of materials that exhibit Bauschinger effect, which in turn serves to reduce the yield strength in compression as a result of prior tensile plastic overload (ref 2).

Three types of steel are addressed herein:

- Two A723 steels with nominal (0.1% offset) yield strengths of 1130 and 1330 MPa.
- HY180 with nominal (0.1% offset) yield strength of 1180 MPa.
- PH 13-8 Mo and PH 13-8 Mo super-tough with nominal (0.1% offset) yield strengths of 1380 and 1355 MPa, respectively.

Details of the experimental testing procedure are given in Reference 3.

The principal features of a uniaxial test for gun steels are illustrated in Figure 1.

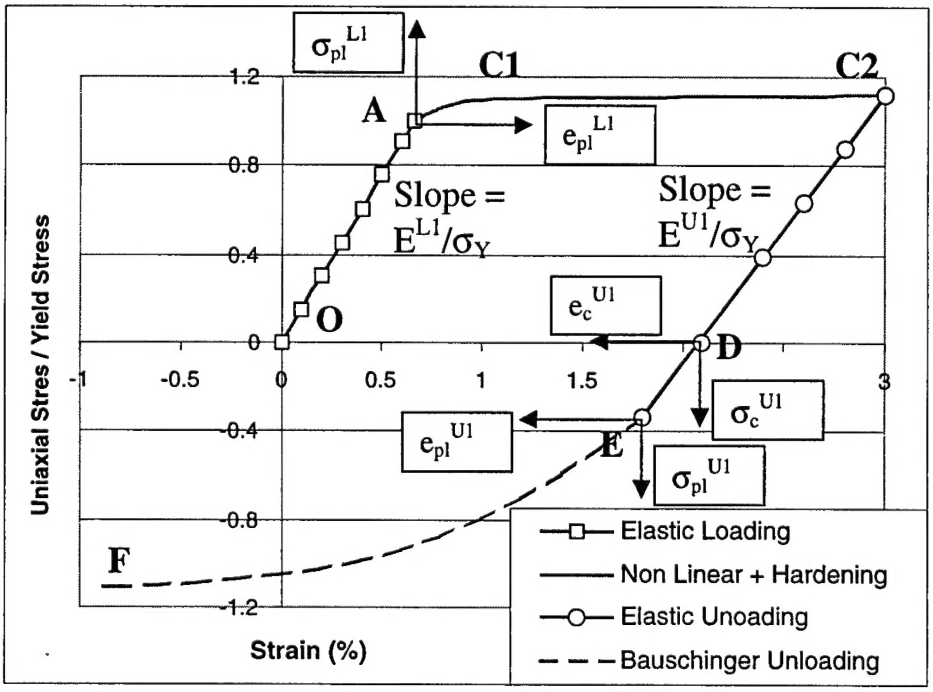

Figure 1. Typical uniaxial stress-strain behavior showing strain hardening, reduced elastic modulus in compression, and Bauschinger effect.

L1 represents an initial tensile loading regime, O-A, during which the steel behaves elastically up to the yield point σ_Y defined by a given percentage offset. The elastic modulus over this range is E^{L1}. The material then behaves plastically, A-C1-C2. This phase may involve significant nonlinearity, A-C1, and predominantly linear strain hardening (or softening), C1-C2. In the case of A723 steel regime, A-C2 is characterized by modest linear strain hardening over a strain range of e_{pl}^{L1}. In the case of HY180, it is characterized by nonlinearity followed by zero strain hardening, reaching a constant value at approximately 3% total strain, whereas 13-8 steels exhibit nonlinearity followed by strain softening.

U1 represents reversal of loading with elastic modulus E^{U1}; this elastic unloading with modulus E^{U1} up to 17% lower than E^{L1} is discussed in Reference 3 and is of importance because it will contribute significantly in subsequent autofrettage residual stress calculations. The tensile (positive) stress reduces and subsequently becomes compressive (negative) at point D but continues to behave elastically up to point E. Thereafter behavior becomes nonlinear, moving asymptotically towards a bound. The value of stress at point E, the onset of nonlinearity, is $-\beta\sigma_Y$ where β is the Bauschinger effect factor (BEF) (ref 2). Both β and the shape of the curve E-F are a strong function of the maximum initial plastic strain e_{pl}^{L1*}.

APPLICATION TO GUN TUBES

When a tube undergoes autofrettage, the equivalent stress within the gun tube follows O-A-C1-C2 during the initial autofrettage pressurization or swage, and C2-D-E-F during the removal of swage or pressure. Hence a family of uniaxial cycles, O-A-C1-C2-D-E-F, each a function of initial plastic strain and hence of radial location, defines equivalent stress for the gun steel during the autofrettage process. This, in turn, with appropriate equilibrium, compatibility, and boundary conditions, is sufficient to calculate numerically the residual stress locked into the tube by autofrettage. Results of such calculations are well documented for the current range of gun steels (refs 4,5), based upon A723 1100 MPa steel, and indeed conform extremely well to the ASME PVP code (ref 6). It is, however, necessary to determine whether the model fits current gun steels in all respects and whether other candidate steels exhibit similar uniaxial behavior. These two issues are examined within this report and an improved model is proposed. Subsequent work will address the numerical modeling and quantification of residual stresses in autofrettaged pressure vessels made from these candidate high-strength steels.

STRAIN RANGES IN TYPICAL GUN TUBES DURING AUTOFRETTAGE

Plastic strains during autofrettage are a strong function of the ratio *autofrettage radius/bore radius* and a weak function of the ratio *outer radius/bore radius* (ref 4). Consider a typical hydraulically autofrettaged gun tube having *outer radius/bore radius* = 2 with 70% overstrain (i.e., *autofrettage radius/bore radius* = 1.7). In this case, using program HENCKY (ref 4), and assuming typical properties for an A723-1100 MPa steel, equivalent strains at the bore and at points 10% into the wall thickness may be calculated. These are listed in Table 1.

Table 1. Percentage Equivalent Strain Values During Autofrettage Loading (L1), and Autofrettage Unloading (U1) at Two Locations Within the Tube Wall (Diameter Ratio = 2.0, 70% Overstrain)

	At Bore	10% Into Wall
Elastic Strain (O-A)	0.531%	0.531%
Plastic Strain (A-C2)	1.054%	0.761%
Elastic Strain (C2-E)	0.621%	0.628%
Plastic Strain (E-F)	0.362%	0.178%

Note the modest, but significant, value of unloading plastic strain, approximately one-third or less of the plastic strain during loading. This serves to emphasize the fact that uniaxial testing, which is intended to be truly analogous to material behavior at the bore of a gun tube, requires only small reverse strains. This would involve unloading to a point roughly one-eighth of the way between points E and F in Figure 1. A good engineering rule of thumb, which applies over the maximum region likely to be affected by further yielding during proof testing, is seen to be a total strain reversal (elastic + plastic) equal to initial plastic strain. Table 1 thus provides uniaxial testing strains that model autofrettage loading and unloading. Any subsequent loading cycle, L2 (e.g., proof testing) must obviously be initiated from a realistically located point F.

The values and locations of plastic strain during autofrettage are illustrated in Figure 2 for a typical tube with 70% overstrain. The maximum extent of reyielding during autofrettage unloading is also shown (24% of wall thickness), as is the maximum extent of reyielding during typical proof testing (13% of wall thickness).

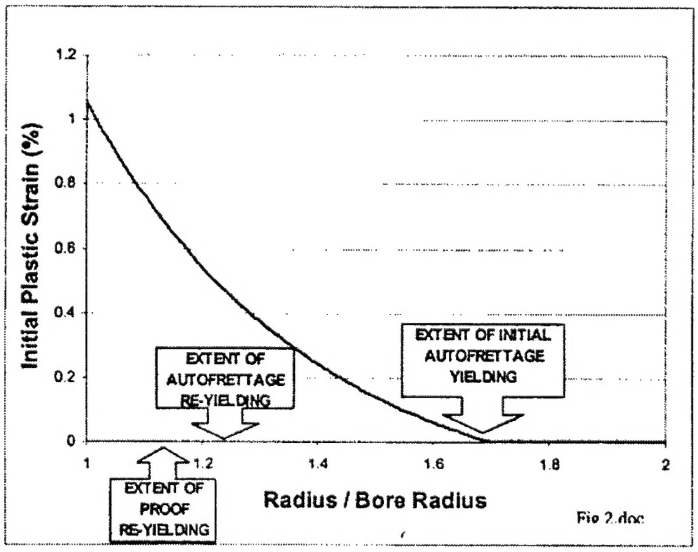

Figure 2. Percentage initial plastic strain during autofrettage loading (continuous line) and maximum extent of initial yielding and reyielding (arrows)(diameter ratio = 2.0, 70% overstrain).

MODELING OF THE INITIAL LOADING PHASE

Linear elastic behavior in Figure 1 is represented as O-A. The plastic phase A-C1-C2 is herein represented as

$$\sigma_{pl}^{L1}/\sigma_Y = a\ Tanh(c\ e_{pl}^{L1}) + d\ e_{pl}^{L1} \qquad (1)$$

The first term models the predominantly nonlinear phase A-C1, while the second term provides linear strain hardening or softening. Hence, for bilinear materials with zero strain hardening $a = d = 0$, for bi-linear with strain hardening $a = 0$, and for nonlinear with zero strain hardening $d = 0$.

MODELING OF THE BAUSCHINGER AFFECTED RANGE

Note that β is reported in earlier experimental work (ref 7) relating to the determination of BEF. The regime D-E-F, interpolated from Reference 7, has been fitted numerically by Parker et al.; see equation (2) in Reference 8. In the current notation this equation becomes

$$\sigma_c^{U1}/\sigma_Y = 0.064113 + 0.34816\ exp(-12.871\ e_{pl}^{L1*})$$
$$+ [1.1619 + 0.5975\ exp(-2.175\ e_{pl}^{L1*})]\ e_c^{U1}$$
$$- [0.54959 + 0.74913\ exp(-9.637\ e_{pl}^{L1*})]\ (e_c^{U1})^2 \qquad (2)$$

Here all strains are expressed as percentage strain and e_{pl}^{L1*} is the maximum percentage plastic strain during prior tensile loading. σ_c^{U1} and e_c^{U1} are total compressive stress and compressive strain, respectively, during cycle U1, i.e., e_c^{U1} is measured horizontally from point D in Figure 1 and σ_c^{U1} is measured vertically. If σ_c^{U1} exceeds the elastic value defined by D-E, the elastic value is assumed.

Equation (2) performs extremely well for current gun steels of up to 1100 MPa nominal yield strength and for the ranges of unloading plastic strain, e_{pl}^{U1}, experienced during hydraulic autofrettage. However, the equation is quadratic in form and is therefore unable to model the asymptotic behavior at high compressive strain shown as a hatched line in Figure 1. The nonlinear kinematic hardening model could, in principle, be used to model σ_c^{U1} over E-F during the unloading cycle U1. This model takes the form (ref 1)

$$\sigma_c^{U1} = \alpha\ tanh(\chi\ .\ e_{pl}^{U1}) + \kappa \qquad (3)$$

where α, χ, and κ are constants for the particular material.

Equation (3) does exhibit an asymptotic behavior at high compressive strain levels. Unfortunately, since κ is analogous to $\beta\sigma_Y$, and β is itself a function of maximum initial plastic strain, e_{pl}^{L1*}, this form of the nonlinear kinematic hardening model cannot incorporate Bauschinger effect. Equation (4) is proposed for improved modeling of the nonlinear region E-F. It incorporates Bauschinger effect and ensures correct asymptotic behavior, including strain hardening, at high reverse strains. Note that both γ and β are assumed to be functions of maximum initial plastic strain, e_{pl}^{L1*}; the form of each of these functions is reported in upcoming sections.

$$\sigma_c^{U1}/\sigma_Y = \{[1 + a - \beta] \,.\, tanh(\gamma \,.\, e_{pl}^{U1})\} + \beta + d \,.\, e_{pl}^{U1} \qquad (4)$$

Since equation (4) must encompass the possibility that the uniaxial specimen is not deformed plastically in tension prior to compressive loading (i.e., $e_{pl}^{L1*} = 0$ giving $\beta = 1$), it is a requirement that

$$\gamma(e_{pl}^{L1*} = 0) = c \qquad (5)$$

which condition is enforced in upcoming numerical fitting procedures.

Rees (ref 9) argues that the only meaningful definition of β is limit of proportionality, rather than the usual choice of offsets such as 0.2, 0.1, or 0.05% in the case of Reference 7. With the benefit of hindsight, it is clear that a very low value of offset is desirable in determining β. An offset value of 0.01% was adopted in analyzing experimental data that then corresponds reasonably well with the implicit values of β for A723 1100 MPa steel determined via equation (1) from its intercept with the equivalent elastic behavior.

One potentially attractive method of determining γ would be to impose continuity of slope E^{U1} at onset of Bauschinger effect at $e_{pl}^{U1} = 0$, by differentiating equation (4) with respect to e_{pl}^{U1}, and thence calculating γ directly. This option was tested but rejected because it did not provide the required high quality of fit over the crucial range following onset of reversed yielding.

EXPERIMENTAL RESULTS AND NUMERICAL FITTING

A723 Steel

Figure 3 shows a typical experimental stress-strain plot from a uniaxial test on A723 1130 MPa steel to 1% total initial strain (ref 3), during L1 and U1 cycles. Figure 4 shows similar data for 3% total initial strain. The principal features described in the introduction are evident.

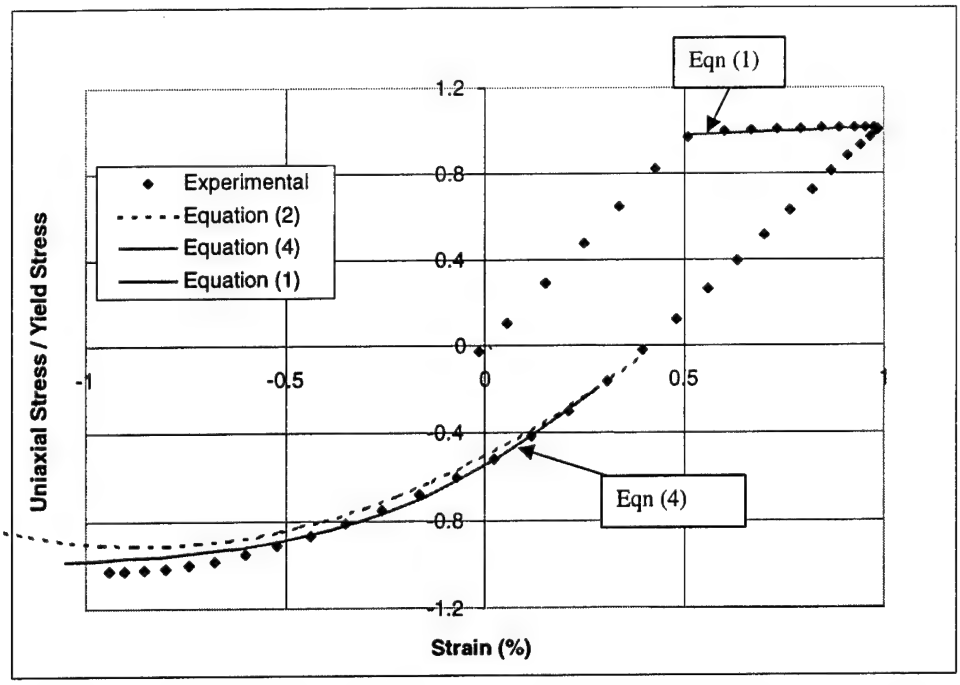

Figure 3. Experimental uniaxial stress-strain data compared with fitting to equation (2) and equations(1) and (4); 1% total initial strain, A723-1130 MPa steel.

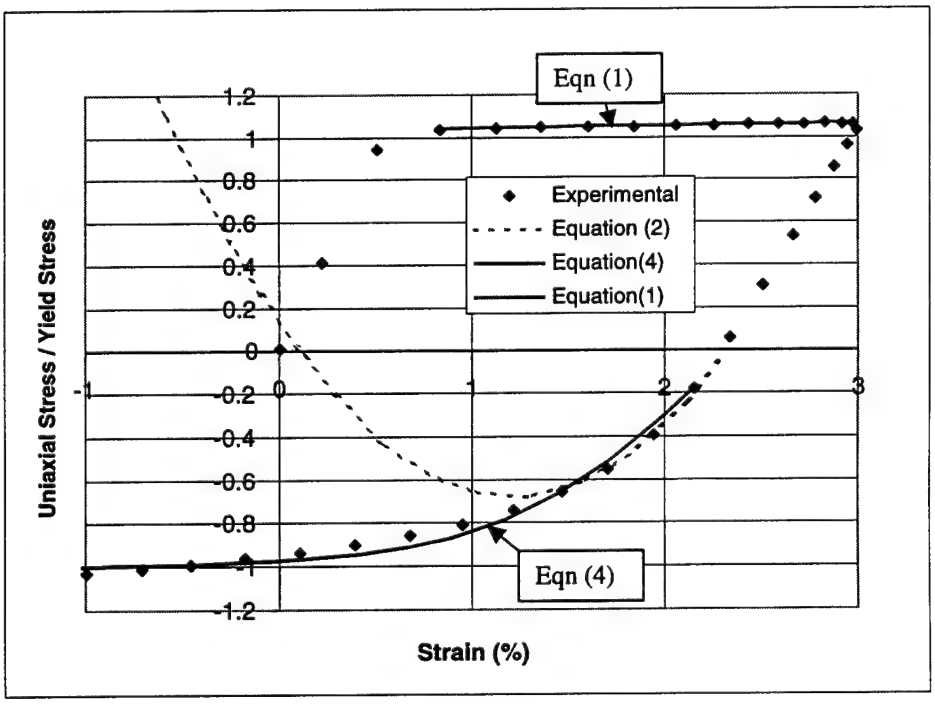

Figure 4. Experimental uniaxial stress-strain data compared with fitting to equation (2) and equations (1) and (4); 3% total initial strain, A723-1130 MPa steel.

Figures 3 and 4 also show the fit, based upon equation (2), to the behavior during reversed yielding. Clearly equation (2) models very well the profile for the strain-ranges encountered during autofrettage (Table 1), but deviates at higher reversed-strains. Figures 3 and 4 also show the fit, based upon equations (1) and (4). β (0.01% offset) was calculated from experimental data and then fitted as a function of e_{pl}^{LI*}. γ was then obtained as a function of e_{pl}^{LI*} from a "best fit" to the full set of individual experimental profiles for each of the steels examined, incorporating the constraint imposed by equation (5). Table 2 shows the numerical fit, including values used in equations (1) and (4), together with mean values of material properties.

Table 2. A723 Steel Numerically Fit to Experimental Data
(Note that e_{pl}^{LI*} is percentage value.)

$a = 0, c = 0, d = 0.013$	A723-1130 MPa
$a = 0, c = 0, d = 0.035$	A723-1380 MPa
$E^{UI}/E^{LI} = 1 - 0.15\ Tanh(1.2\ e_{pl}^{LI*})$	
$\beta = 0.1684\ [Tanh(1 - e_{pl}^{LI*})]^{3.6} + 0.17 \quad e_{pl}^{LI} <= 1$	
$\beta = 0.17 \quad e_{pl}^{LI} > 1$	
$\gamma = 1.2858\ (e_{pl}^{LI*})^{(-0.323)}$	A723-1130 MPa
$\gamma = 1.1244\ (e_{pl}^{LI*})^{(-0.3455)}$	A723-1380 MPa
Material Properties (Mean Values)	
σ_Y (0.1%) = 1139 MPa, E_{LI} = 209 GPa	A723-1130 MPa
σ_Y (0.1%) = 1344 MPa, E_{LI} = 203 GPa	A723-1380 MPa

HY180 Steel

In the case of HY180 steel, the nonlinearity of the initial plastic loading phase requires an appropriate numerical fit, whereas the linear strain hardening is zero. Furthermore, 0.05% offset definition of initial yield is required to obtain a satisfactory fit. Table 3 shows the numerical fit, including values used in equations (1) and (4), together with mean values of material properties.

Table 3. HY180 Steel Numerically Fit to Experimental Data
(Note that e_{pl}^{LI*} is percentage value.)

$a = 0.231, c = 2, d = 0$
$E^{UI}/E^{LI} = 1 - 0.17\ Tanh(1.2\ e_{pl}^{LI*})$
$\beta = 1 - 0.832\ Tanh(0.85\ e_{pl}^{LI*})$
$\gamma = 2 - 1.3\ Tanh(0.6\ e_{pl}^{LI*})$
Material Properties (Mean Values)
σ_Y (0.05%) = 1169 MPa, E^{LI} = 201.9 GPa

Figures 5 and 6 show experimental results for 1. and 4% total strain compared with proposed numerical fit.

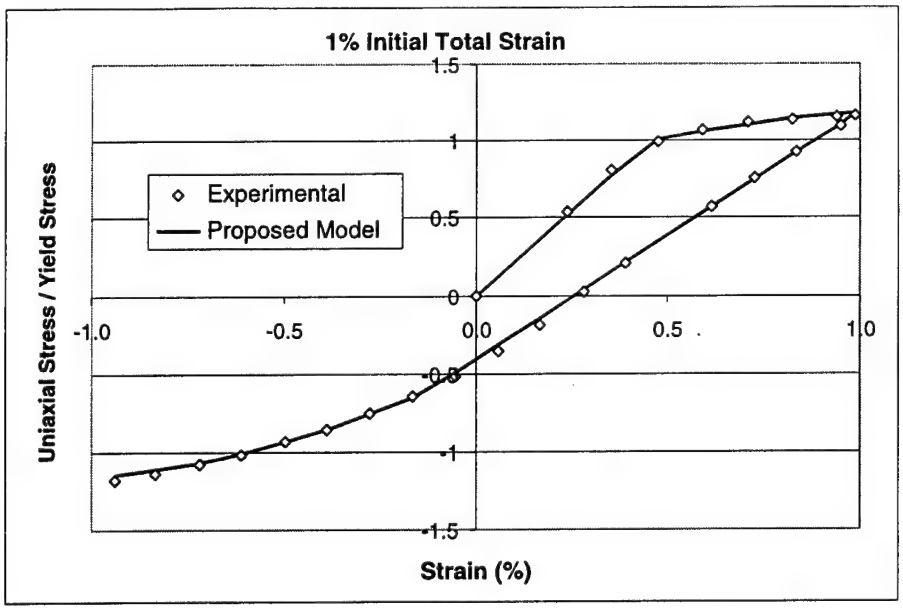

Figure 5. Experimental uniaxial stress-strain data compared with fitting to equations (1) and (4) and to modulus ratio; 1% total initial strain, HY180 steel.

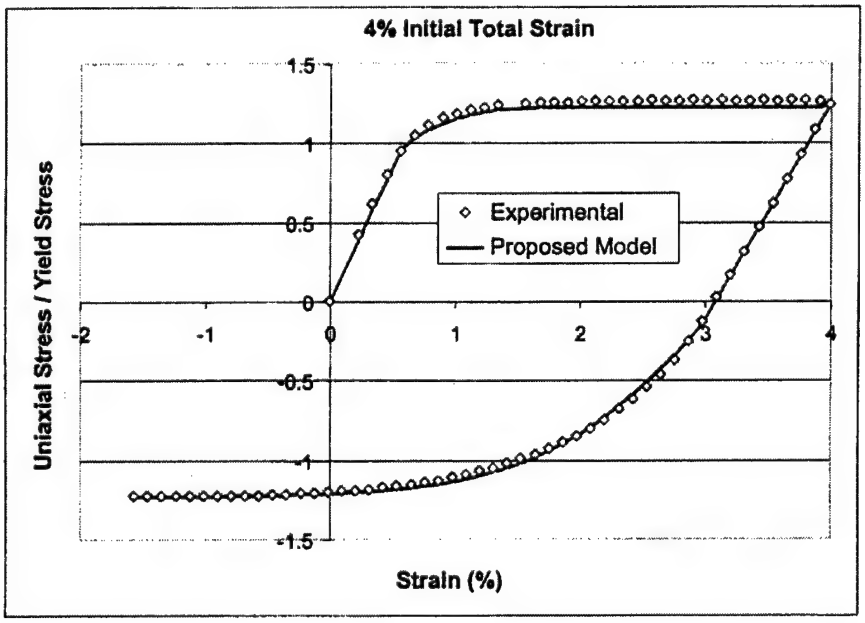

Figure 6. Experimental uniaxial stress-strain data compared with fitting to equations (1) and (4) and to modulus ratio; 4% total initial strain, HY180 steel.

PH 13-8 Mo Steels

In the case of PH 13-8 Mo steels, there is nonlinearity of the initial plastic loading phase that requires an appropriate numerical fit, and the 0.05% offset definition of initial yield is again required to obtain a satisfactory fit. Strain softening is evident. Table 4 shows the numerical fit, including values used in equations (1) and (4), together with mean values of material properties.

Table 4. PH 13-8 Mo Steels Numerically Fit to Experimental Data
(Note that e_{pl}^{LI*} is percentage value.)

$a = 0.085$, $c = 3.9$, $d = -0.009$ $E^{UI}/E^{LI} = 1 - 0.09221\ e_{pl}^{LI*} + 0.0083\ (e_{pl}^{LI*})^2$
$\beta = 1 - 0.85*Tanh(4\ e_{pl}^{LI*})$ $\gamma = 3.9 - 3.01*Tanh(3*\ e_{pl}^{LI*})$
Material Properties (Mean Values) σ_Y (0.05%) = 1346 MPa, E^{LI} = 206 GPa PH 13-8 Mo σ_Y (0.05%) = 1302 MPa, E^{LI} = 195 GPa PH 13-8 Mo Super-Tough

Figures 7 and 8 show experimental results for 2 and 3% total initial tensile strain compared with proposed numerical fit. Note that two types of PH 13-8 Mo steel were examined. While the expressions in Table 4 adequately represent the normalized fit for both types, there was a significant difference in the mean values of 0.05% offset yield strength. This effect will be of significance in future work involving calculation of autofrettage residual stresses for the two types of PH 13-8 Mo steel.

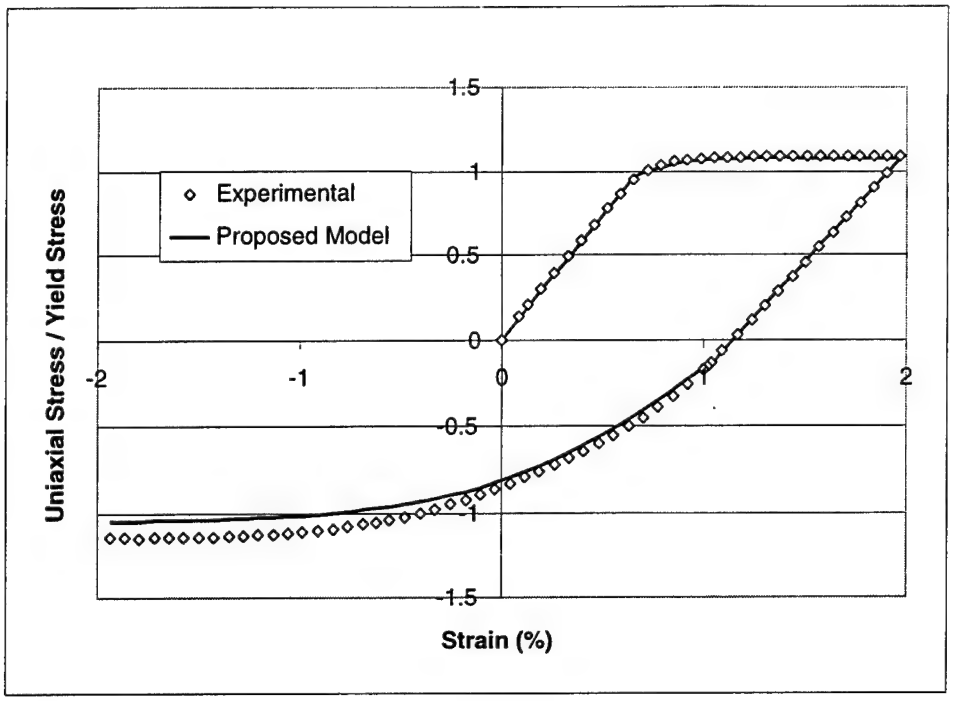

Figure 7. Experimental uniaxial stress-strain data compared with fitting to equations (1) and (4) and to modulus ratio; 2% total initial strain, PH 13-8 Mo steel.

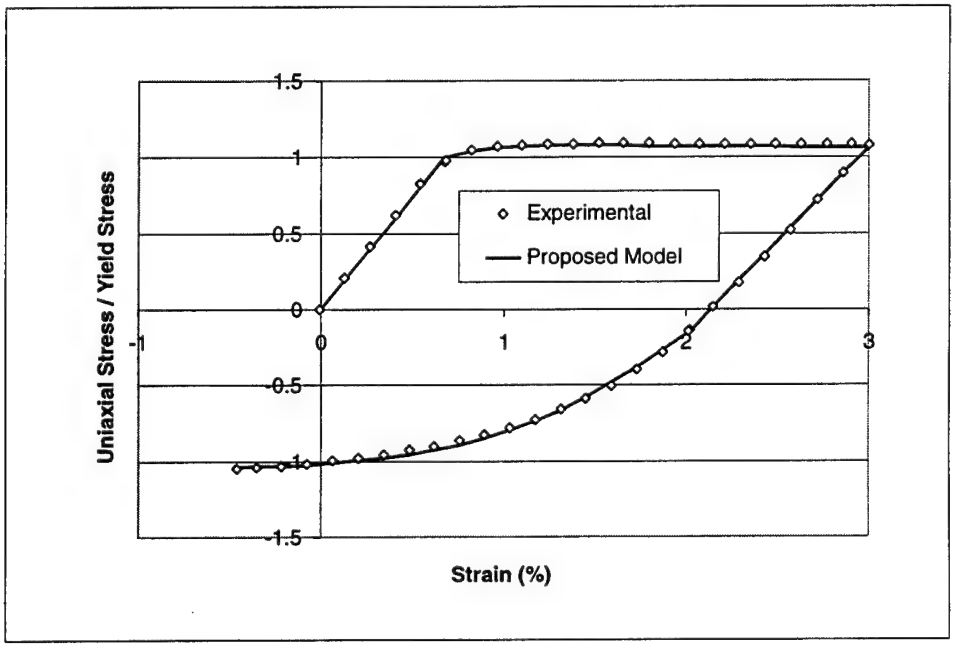

Figure 8. Experimental uniaxial stress-strain data compared with fitting to equations (1) and (4) and to modulus ratio; 3% total initial strain, PH 13-8 Mo super-tough steel.

CONCLUSIONS AND FUTURE WORK

Gun steels have been subjected to a series of uniaxial tests. These tests are intended to provide equivalent stress data for input to subsequent numerical analyses. The steels are A723-1130 MPa (nominal) yield strength and possible alternatives, namely A723-1380 MPa (nominal) yield strength, HY80-1180 MPa (nominal) yield strength, PH 13-8 Mo and PH 13-8 Mo super-tough.

For each steel the experimental data during initial and reversed loading can be fitted with considerable accuracy using a new variant of the nonlinear kinematic hardening model that includes Bauschinger effect as a function of prior tensile plastic strain. This new variant provides an excellent fit within the strain ranges experienced in real gun tubes during autofrettage. It also provides the desired asymptotic behavior at much higher reverse-strain levels and therefore represents an improvement over previous models.

Future work will encompass:

- Calculation of residual stress profiles and associated fatigue lifetimes in tubes made from the candidate steels.
- Prediction of onset of reyielding during proof testing.
- Detailed prediction of nonlinear strain behavior during typical proof testing and firing. This may, in turn, lead to a reassessment of the safe maximum pressure calculation for autofrettaged tubes.

REFERENCES

1. Lemaitre, J., and Chaboche, J.-L., *Mechanics of Solid Materials*, Cambridge University Press, 1990.

2. Bauschinger, J., 1881, "Ueber die Veranderung der Elasticitatagrenze und dea Elasticitatamoduls Verschiadener Metalle," *Zivilingenieur*, Vol. 27, 1881, Columns 289-348.

3. Troiano, E., Parker, A.P., Underwood, J.H., and Mossey, C., 2001, "Experimental Data, Numerical Fit, and Life Approximations Relating to the Bauschinger Effect in High-Strength Armament Steels," to be published.

4. Parker, A. P., 2001, "Autofrettage of Open-End Tubes – Pressures, Stresses, Strains and Code Comparisons," *Transactions of the ASME, Journal of Pressure Vessel Technology,* Vol. 123, 2001, pp. 271-281.

5. Chakrabarty, J., *Theory of Plasticity*, McGraw Hill, NY, 1987.

6. "Design Using Autofrettage," *ASME Pressure Vessel and Piping Design Code*, Division 3, Section 8, Article KD-5, 1997, pp. 71-73.

7. Milligan, R.V., Koo, W.H., and Davidson, T.E., "The Bauschinger Effect in a High Strength Steel," *Transactions of the ASME D*, 1966, pp. 480-488.

8. Parker, A.P., Underwood, J.H., and Kendall, D.P., "Bauschinger Effect Design Procedures for Autofrettaged Tubes Including Material Removal and Sachs' Method," *Transactions of the ASME, Journal of Pressure Vessel Technology,* Vol. 121, 1999, pp. 430-437.

9. Rees, D.W.A., "Anisotropic Hardening Theory and the Bauschinger Effect," *Journal of Strain Analysis*, Vol. 16, No. 2, 1981, pp. 85-95.

NOMENCLATURE

a, c, d	Coefficients in equation (1) relating to initial plastic deformation
e_c^{UI}	Total compressive strain during reversed loading
e_{pl}^{LI}	Plastic strain during initial plastic deformation
e_{pl}^{LI*}	Maximum plastic strain during initial plastic deformation
e_{pl}^{UI}	Nonlinear strain during reversed loading
E^{LI}	Elastic modulus during initial tensile loading
E^{UI}	Elastic modulus during initial load reversal
α, χ, κ	Traditional nonlinear kinematic hardening coefficients
β	Bauschinger effect factor, function of e_{pl}^{LI*}
γ	Proposed nonlinear kinematic hardening, function of e_{pl}^{LI*}
σ_{pl}^{LI}	Stress during initial plastic deformation
σ_c^{UI}	Total compressive stress during reversed loading
σ_{pl}^{UI}	Nonlinear stress during reversed loading
σ_Y	Material yield stress obtained from given offset

TECHNICAL REPORT INTERNAL DISTRIBUTION LIST

	NO. OF COPIES
TECHNICAL LIBRARY ATTN: AMSTA-AR-CCB-O	5
TECHNICAL PUBLICATIONS & EDITING SECTION ATTN: AMSTA-AR-CCB-O	3
OPERATIONS DIRECTORATE ATTN: SIOWV-ODP-P	1
DIRECTOR, PROCUREMENT & CONTRACTING DIRECTORATE ATTN: SIOWV-PP	1
DIRECTOR, PRODUCT ASSURANCE & TEST DIRECTORATE ATTN: SIOWV-QA	1

NOTE: PLEASE NOTIFY DIRECTOR, BENÉT LABORATORIES, ATTN: AMSTA-AR-CCB-O OF ADDRESS CHANGES.

TECHNICAL REPORT EXTERNAL DISTRIBUTION LIST

	NO. OF COPIES
DEFENSE TECHNICAL INFO CENTER ATTN: DTIC-OCA (ACQUISITIONS) 8725 JOHN J. KINGMAN ROAD STE 0944 FT. BELVOIR, VA 22060-6218	2
COMMANDER U.S. ARMY ARDEC ATTN: AMSTA-AR-WEE, BLDG. 3022	1
AMSTA-AR-AET-O, BLDG. 183	1
AMSTA-AR-FSA, BLDG. 61	1
AMSTA-AR-FSX	1
AMSTA-AR-FSA-M, BLDG. 61 SO	1
AMSTA-AR-WEL-TL, BLDG. 59 PICATINNY ARSENAL, NJ 07806-5000	2
DIRECTOR U.S. ARMY RESEARCH LABORATORY ATTN: AMSRL-DD-T, BLDG. 305 ABERDEEN PROVING GROUND, MD 21005-5066	1
DIRECTOR U.S. ARMY RESEARCH LABORATORY ATTN: AMSRL-WM-MB (DR. B. BURNS) ABERDEEN PROVING GROUND, MD 21005-5066	1
COMMANDER U.S. ARMY RESEARCH OFFICE ATTN: TECHNICAL LIBRARIAN P.O. BOX 12211 4300 S. MIAMI BOULEVARD RESEARCH TRIANGLE PARK, NC 27709-2211	1
COMMANDER ROCK ISLAND ARSENAL ATTN: SIORI-SEM-L ROCK ISLAND, IL 61299-5001	1
COMMANDER U.S. ARMY TANK-AUTMV R&D COMMAND ATTN: AMSTA-DDL (TECH LIBRARY) WARREN, MI 48397-5000	1
COMMANDER U.S. MILITARY ACADEMY ATTN: DEPT OF CIVIL & MECH ENGR WEST POINT, NY 10966-1792	1
U.S. ARMY AVIATION AND MISSILE COM REDSTONE SCIENTIFIC INFO CENTER ATTN: AMSAM-RD-OB-R (DOCUMENTS) REDSTONE ARSENAL, AL 35898-5000	2
COMMANDER U.S. ARMY FOREIGN SCI & TECH CENTER ATTN: DRXST-SD 220 7TH STREET, N.E. CHARLOTTESVILLE, VA 22901	1

NOTE: PLEASE NOTIFY COMMANDER, ARMAMENT RESEARCH, DEVELOPMENT, AND ENGINEERING CENTER, BENÉT LABORATORIES, CCAC, U.S. ARMY TANK-AUTOMOTIVE AND ARMAMENTS COMMAND, AMSTA-AR-CCB-O, WATERVLIET, NY 12189-4050 OF ADDRESS CHANGES.

DEPARTMENT OF THE ARMY
ARMAMENT RESEARCH, DEVELOPMENT AND ENGINEERING CENTER
BENÉT LABORATORIES, CCAC
US ARMY TANK-AUTOMOTIVE AND ARMAMENTS COMMAND
WATERVLIET, NY 12189-4000

OFFICIAL BUSINESS
AMSTA-AR-CCB-O
TECHNICAL LIBRARY